Stem Cell Research (2015) 14, 105–113

Available online at www.sciencedirect.com

ScienceDirect

www.elsevier.com/locate/scr

Cryosectioning the intestinal crypt-villus axis: An ex vivo method to study the dynamics of epigenetic modifications from stem cells to differentiated cells

Audrey Vincent[a,b,c,*], Catherine Kazmierczak[a,b,c,d], Belinda Duchêne[a,b,c], Nicolas Jonckheere[a,b,c], Emmanuelle Leteurtre[a,b,c,d], Isabelle Van Seuningen[a,b,c]

[a] *Inserm, UMR837, Jean Pierre Aubert Research Center (JPARC), Team 5 "Mucins, Epithelial Differentiation and Carcinogenesis," rue Polonovski, Lille, France*
[b] *Université Lille 2 Droit et Santé, Lille, France*
[c] *Centre Hospitalier Régional et Universitaire de Lille, Lille, France*
[d] *Centre de Biologie Pathologie, CHRU Lille, Lille, France*

Received 26 September 2014; received in revised form 26 November 2014; accepted 12 December 2014
Available online 27 December 2014

Abstract The intestinal epithelium is a particularly attractive biological adult model to study epigenetic mechanisms driving adult stem cell renewal and cell differentiation. Since epigenetic modifications are dynamic, we have developed an original *ex vivo* approach to study the expression and epigenetic profiles of key genes associated with either intestinal cell pluripotency or differentiation by isolating cryosections of the intestinal crypt-villus axis. Gene expression, DNA methylation and histone modifications were studied by qRT-PCR, methylation-specific PCR and micro-chromatin immunoprecipitation, respectively. Using this approach, it was possible to identify segment-specific methylation and chromatin profiles. We show that (i) expression of intestinal stem cell markers (*Lgr5*, *Ascl2*) exclusively in the crypt is associated with active histone marks, (ii) promoters of all pluripotency genes studied and transcription factors involved in intestinal cell fate (*Cdx2*) harbour a bivalent chromatin pattern in the crypts and (iii) expression of differentiation markers (*Muc2*, *Sox9*) along the crypt-villus axis is associated with DNA methylation. Hence, using an original model of cryosectioning along the crypt-villus axis that allows *in situ* detection of dynamic epigenetic modifications, we demonstrate that regulation of pluripotency and differentiation markers in healthy intestinal mucosa involves different and specific epigenetic mechanisms.

* Corresponding author at: Inserm UMR837, Jean-Pierre Aubert Research Center, Team 5 "Mucins, Epithelial Differentiation and Carcinogenesis," Rue Polonovski, Lille 59045, France.
E-mail address: audrey.vincent@inserm.fr (A. Vincent).

http://dx.doi.org/10.1016/j.scr.2014.12.002
1873-5061/

Introduction

Cell differentiation in adults involves flexible but precise control of the expression of genes specific for each cell fate or pluripotency. Crucial changes in their expression are most likely controlled by specific epigenetic rearrangements (Vincent & Van Seuningen, 2009). Extensive studies conducted to characterise embryonic stem cells (ESC) at the epigenetic level have shown that ESC harbour a permissive chromatin with hypomethylation of their genome compared to differentiated cells (Bibikova et al., 2006) and bivalent histone marks where large regions containing trimethylated K27H3 (gene silencing) colocalise with smaller regions containing methylated K4H3 (gene activation) (Bernstein et al., 2006). This allows rapid transcriptional activation of genes specific for a cell fate. One can hypothesise that the plasticity of adult SC involves similar epigenetic mechanisms. However, only a few studies mostly conducted *in vitro* have addressed this concept.

The intestinal epithelium is a particularly attractive biological adult model to study epigenetic mechanisms driving differentiation *in vivo*. In the intestinal epithelium, two populations of SC have already been described and isolated (Lgr5+ and Bmi1+ cells; Barker et al., 2007; Sangiorgi & Capecchi, 2008). Epithelial cell turnover in the intestine is particularly fast and occurs from a well-identified structure, the so-called niche, which provides an optimal microenvironment for SC ensured by epithelial and mesenchymal cells and extracellular substrates (Scoville et al., 2008). Therefore, the intestinal crypt has been defined as a perfect prototype SC compartment (Clevers, 2013a) and is a model of choice to study epigenetic mechanisms involved in adult epithelial cell differentiation. In a recent study based on cell sorting of labelled SC, fifty differentially methylated regions have been identified as driving intestinal SC (ISC) differentiation (Kaaij et al., 2013). Similarly, numerous studies aiming at deciphering cell differentiation mechanisms have been performed either after cell sorting, following *in vitro* culture of SC forced to engage in specific lineages (Pennarossa et al., 2013), or after fractionation methods used to isolate enriched cell subpopulations (Barnard et al., 1989). However, epigenetic profiles are very dynamic and can be profoundly modified during cell culture (Allegrucci et al., 2007) or through cell sorting. Moreover, the lack of reliable tools to isolate ISC forced investigators to avoid the use of specific antibodies by using genetically modified mouse models, where ISC carry fluorescent labels (Wang et al., 2013; Ramalingam et al., 2012). These models were very informative since they already pointed out some epigenetic modifications that are crucial (Sheaffer et al., 2014) or even dispensable (Ho et al., 2013) for intestinal epithelial cell differentiation. However, they may not reflect the progressive epigenetic changes necessary for differentiation programming *in vivo*, especially in humans where these labelling approaches cannot be applied.

In order to circumvent these pitfalls, we have developed an original *ex vivo* method allowing precise cryosectioning of the whole intestinal crypt-villus (CV) axis. This method allowed us (i) to establish the expression and epigenetic profiles of key genes associated with either intestinal cell pluripotency or differentiation and (ii) to show that specific epigenetic programs are engaged in these processes.

Material and methods

Sample collection and cryosectioning the CV axis

All procedures were in accordance with the guideline of animal care committee (Comité Ethique Expérimentation Animale Nord Pas-de-Calais, CEEA75). The distal small intestine from wild-type C57BL/6 mice was collected, separated from mesenteric residues, rinsed in 1× phosphate-buffered saline (PBS), sectioned into pieces of 1 cm in length and opened longitudinally with special intestine scissors (FST 14080-11) to avoid tearing. These small intestine fragments were uniformly flattened with the villi pointing upwards in a 15 × 15 × 5mm Tissue-Tek® cryomold® mold and covered with tissue freezing medium (O.C.T.) (Fig. 1A) before immediate snap-freezing in isopentane cooled at −80 °C (SnapFrost® 80, Alphelys) to avoid cell and nucleus wall damages upon freezing. Frozen tissue blocks were placed on the tissue holder of a cryostat at −20 °C with the villi pointed downwards. The specimen head was oriented in order to section the tissue transversely at 10 μm thickness from the muscular layer through the mucosa until the top of the villi. Four consecutive sections were used as one sample and referred to as one "layer" of the CV axis. Each of the 13 layers of one tissue block was then used either for RNA, DNA extraction or for micro-Chromatin ImmunoPrecipitation assays (μChIP). Between each 40 μm-layer, one 5 μm-section was mounted and stained with standard hematoxylin and eosin (HE) in order to check for crypt and villus morphology, right sectioning progression along the CV axis (muscular layer, crypt bottoms, crypts, CV junctions, villi and top of the villi) and anatomic consistency between the layers of independent tissue blocks (Fig. 1C).

RNA isolation

Total RNA was extracted from each of the layers of one tissue block using the NucleoSpin RNA XS Kit (Macherey-Nagel) following the manufacturer's protocol. Total RNA yields varied in average from approximately 140 ng in samples corresponding to bottom and top layers, where cells are sparse, to 5.9 μg in samples corresponding to intermediate layers. The layers of at least three tissue blocks collected from different mice were independently used for expression profile studies along the CV axis.

Quantitative reverse transcription polymerase chain reaction (qRT-PCR)

Total RNA (140–500 ng) were reverse transcribed using random hexamers (1 μl) and recombinant RT Moloney Murine Leukemia Virus (M-MLV) (Promega). cDNAs were quantified using the SsoFast EvaGreen supermix (Bio-Rad). qRT-PCR was performed on a Bio-Rad CFX96 real-time thermocycler. Primer sequences are listed in Table S1. Fold changes were calculated according to the $2^{-\Delta\Delta Ct}$ method where *GUSB*, and *TBP* housekeeping genes were used for normalisation and the sample corresponding to the bottom of the crypt was used as a reference.

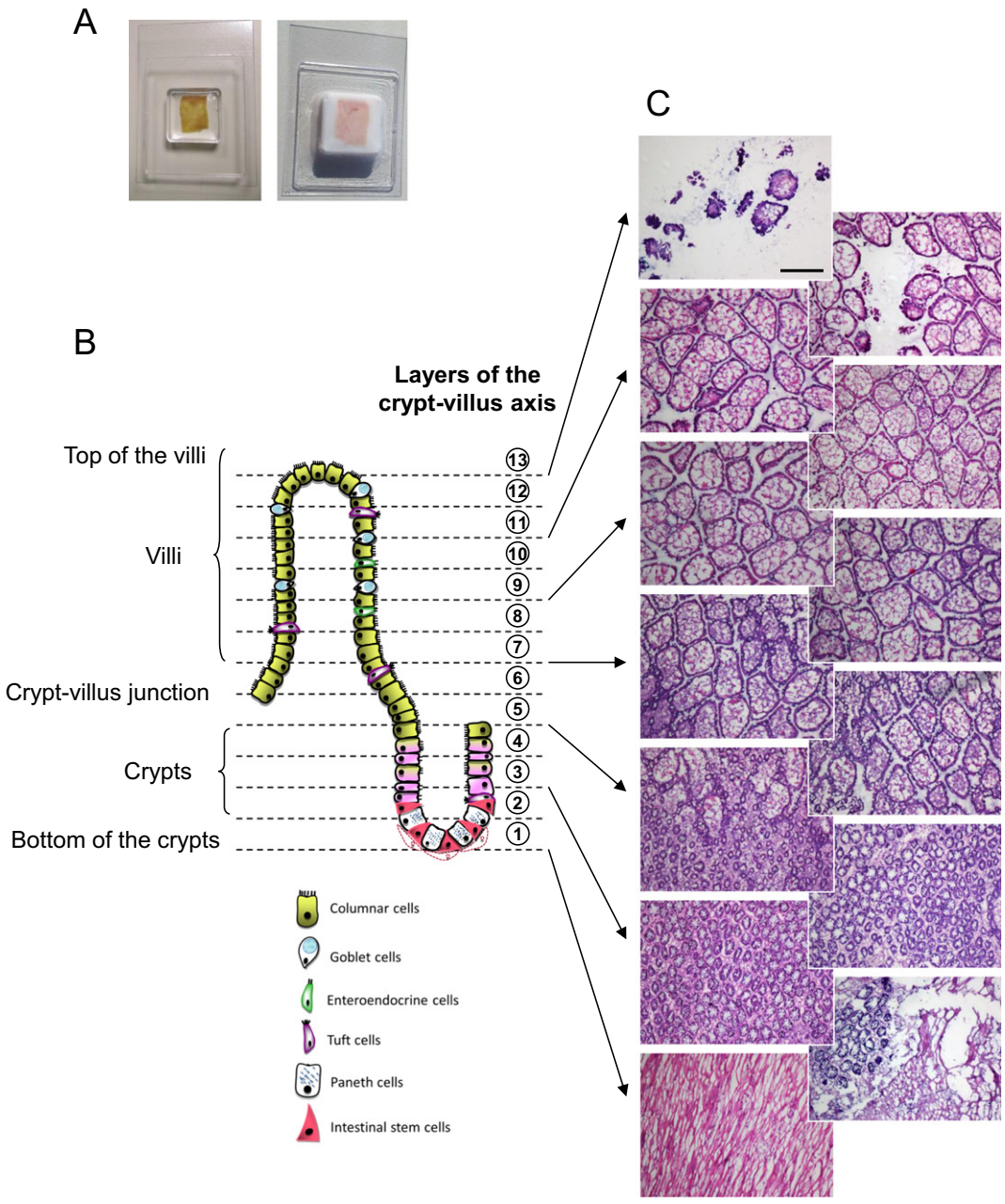

Figure 1 Cryosectioning the CV axis. (A) Photographs representing the flattened intestinal mucosa in a cryomold before and after snap-freezing. (B) Schematic representation of the intestinal mucosa delineated into crypts and villi. Numbers represent each layer or sample, constituted of four consecutive 10 μm cryosections. Discontinued line represents the 5 μm-cryosections used for examination by light microscopy of the morphology and progression along the CV axis on a slide stained with standard HE (C). Magnification ×100. The scale bar indicates 200 μm.

DNA isolation

Genomic DNA was extracted from each of the layers of one tissue block using the NucleoSpin DNA XS Kit (Macherey-Nagel) following the manufacturer's protocol. Total DNA yields varied in average from approximately 880 ng in samples corresponding to bottom and top layers where cells are sparse to 6.9 μg in samples corresponding to intermediate layers. The layers of at least three tissue blocks collected from different mice were independently used for DNA methylation profile studies along the CV axis.

Methylation-specific PCR (MSP)

The methylation status of target gene promoters was determined by MSP as previously described (Vincent et al., 2011) using specific primers for methylated and unmethylated DNA

(listed in Table S2). DNA treated with *Sss*I methylase (New England Biochemicals) and whole-genome amplified DNA (REPLI-g Mini Kit, Qiagen) were used as controls for methylated and unmethylated DNA, respectively. Samples harbouring amplifications with both methylated and unmethylated specific primers were considered partially methylated.

Micro-chromatin immunoprecipitation assays

Fresh pieces of small intestine (~1 cm^2) were fixed in formaldehyde 1% (v/v) in 1× PBS containing complete protease inhibitor cocktail tablets (Roche) for 10 min at room temperature. Fixation was stopped with 0.125 M glycine, and the tissues were rinsed with 1× PBS containing complete protease inhibitor cocktail tablets (Roche) before snap-freezing and cryosectioning as described above.

Each selected 40 μm layer of the CV axis of one tissue block was incubated for 10 min on ice in 100 μl of the tL1 lysis buffer from the True μChIP Kit (Diagenode) containing a provided protease inhibitor cocktail. Three volumes of HBSS were then added before chromatin shearing using the Bioruptor® (24 cycles, 30 s on, 30 s off, Diagenode). Sheared chromatin was separated from cell debris through centrifugation (14 000 ×*g*, 10 min, 4 °C), and optimal size was monitored in a 1.5% (v/v) agarose gel run in 1× sodium borate buffer in the presence of ethidium bromide.

Sheared chromatin was diluted v/v in ChIP Buffer tC1 (True μChIP Kit) according to Diagenode's instructions and divided into four equal aliquots. Two were used for immunoprecipitation at 4 °C on a rotating wheel for 16 h with specific antibodies (0.25 μg for 0.1 A_{260nm}) against either H3K9 (pAb-056-050, Diagenode), H3K27 (#39155, Active Motif) or H3K4 (True μChIP Kit, Diagenode) trimethylation were used. A third aliquot was used for immunoprecipitation with the same amount of rabbit IgGs (Millipore) as a negative enrichment control. The fourth aliquot was set aside as the input sample and kept overnight at −20 °C until purification. Prewashed magnetic beads (True μChIP Kit, Diagenode) were used to capture the immunoprecipitated chromatin and washed with provided buffers according to the manufacturer's instructions. After the last wash with tW4 buffer, immunoprecipitated chromatin was eluted from the True μChIP beads using 120 μl of freshly prepared elution buffer from the I-Pure Kit (Diagenode) and incubated at 65 °C overnight for reverse cross-linking along with the input sample. Immunoprecipitated and input samples were then purified according to the manufacturer's instructions and eluted with 25 μl of provided elution buffer C (I-Pure Kit, Diagenode). The presence of histone marks on target gene promoters was directly assessed using 2 μl of the sample into a 20 μl qPCR reaction using the SsoFast EvaGreen supermix (Bio-Rad) on a Bio-Rad CFX96 real-time thermocycler. Primers are listed in Table S3. Fold enrichments for each layer were calculated according to the $2^{-\Delta\Delta Ct}$ method where the input sample was used for normalisation and the sample immunoprecipitated with the control IgGs was used as the reference.

Results and discussion

Cryosections of the CV axis reflect the gradients of expression of SC and differentiation markers

HE staining of the different segments following cryosectioning confirmed the morphological evolution and cell distribution along the CV axis (Fig. 1B). Expression of SC markers *Lgr5* and *Bmi1* was found mainly at the bottom of the crypt and decreased progressively toward the CV junction to become virtually absent from the villi (Fig. 2A). Putative SC marker *Ascl2* showed a comparable profile with a small increase of expression at the CV junction compared to the bottom of the crypt indicating that *Ascl2* may be a progenitor marker rather than a true SC marker. These results confirm their expression profile previously described (Itzkovitz et al., 2012).

As expected, *Sox9*, which encodes a transcription factor playing roles in intestinal epithelial cell fate including terminal differentiation of the secretory lineage and SC maintenance (Mori-Akiyama et al., 2007), was overexpressed in the crypts compared to the villi (Fig. 3A). The expression study of *Cdx2* which encodes a transcription factor involved in epithelial cell terminal differentiation (Chawengsaksophak et al., 1997) (Fig. 3A) and one of its transcriptional targets (Benoit et al., 2010), *Sis* encoding the absorptive lineage marker sucrase isomaltase (Fig. S2), showed that they were mostly found in the villi and the top of the villi while they were largely underrepresented in the crypts until the CV junction. Similarly, we found that *Casp3*, which encodes a caspase involved in the shedding of differentiated cells by apoptosis at the top of the villi (Grossmann et al., 2002), was gradually expressed from the bottom of the crypt to the top of the villi (Fig. S2).

Muc2, which encodes a goblet cell marker and the major component of intestinal mucus (Tytgat et al., 1994), was inconstantly expressed along the CV axis (Fig. 3A). This is concordant with the fact that goblet cells are disseminated along the CV axis and only represent about 10% of the intestinal epithelium. Interestingly, *Muc2* was also highly expressed at the bottom of the crypts, where goblet cells are not fully differentiated. This is in accordance with our previous findings showing that *Muc2* mRNAs are found at the bottom of the crypts early during mouse and human development, before terminal differentiation of goblet cells (Buisine et al., 2000).

Finally, we found that while *ChgA*, which encodes the neuroendocrine cell marker Chromogranin A, was uniformly expressed along the CV axis, *Defa24*, which encodes the Paneth cell marker Defensin alpha 24, was 7-fold overexpressed in the crypt segments compared to the strict bottom of the crypt and was decreased in the layers corresponding to the villi (Fig. S2). These data are concordant with the distribution of neuroendocrine cells and Paneth cells, which are found either equally distributed along the CV axis or exclusively in the crypts, respectively.

Altogether these results validate our cryosectioning method since we confirmed the previously described gradients of expression of genes involved either in stemness and pluripotency or in absorptive and secretory lineages of the mouse intestinal mucosa.

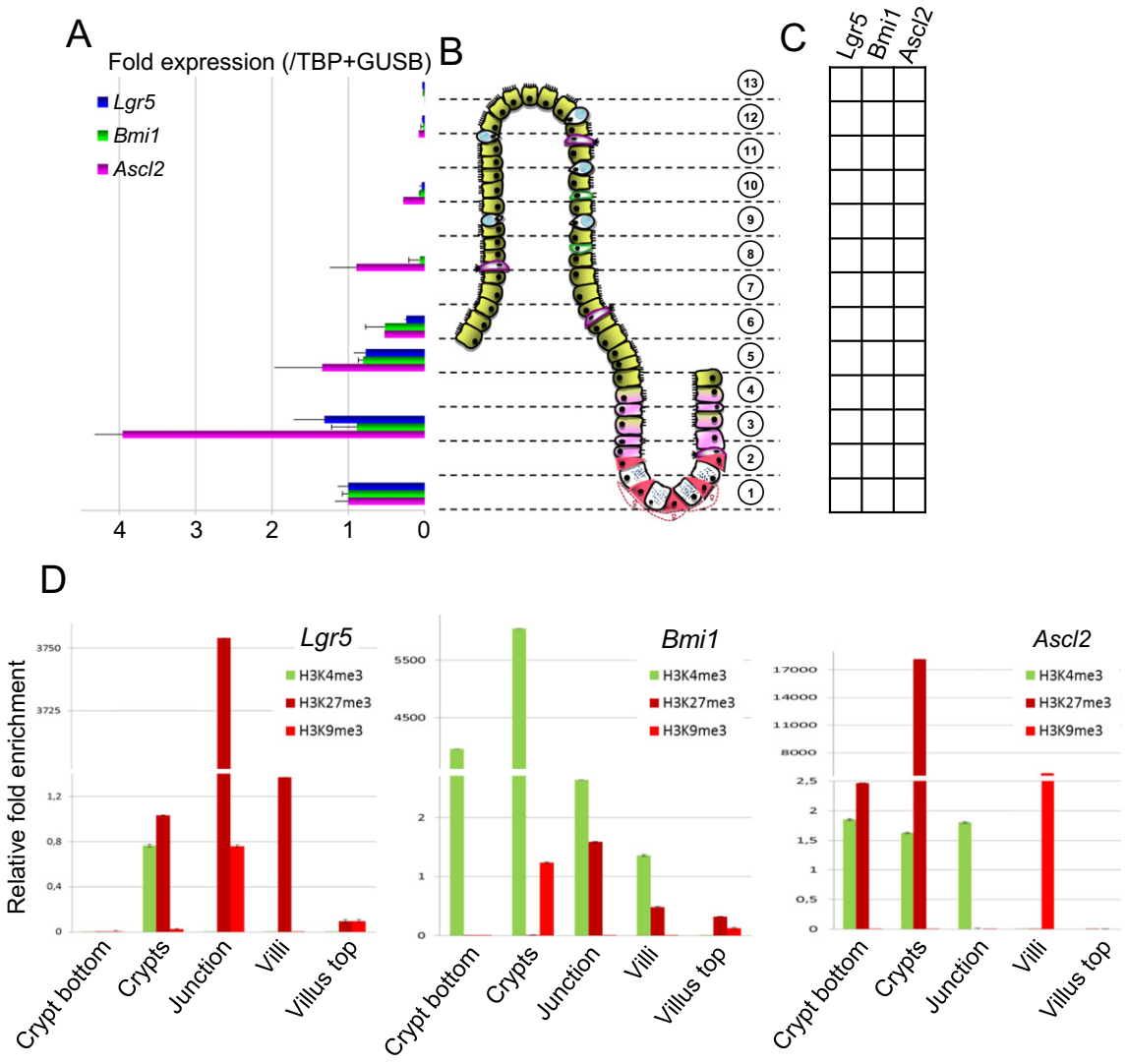

Figure 2 Transcriptional and epigenetic profile of SC markers along the CV axis. (A) Expression profile in each layer of the CV axis of one tissue block was studied by qRT-PCR. Graphs represent relative expression normalised with the housekeeping genes *GUSB* and *TBP*. The sample corresponding to the bottom of the crypt was used as a reference and fold changes were calculated according to the $2^{-\Delta\Delta Ct}$ method. Error bars represent technical replicates of each layer of one tissue block. (B) Schematic representation of the intestinal mucosa delineated into the 13 40 μm-layers of the CV axis that were used either for mRNA expression, MSP or ChIP analysis. (C) DNA methylation profile in each layer of the CV axis at promoters of SC markers was studied by MSP. White boxes indicate the absence of DNA methylation in a layer (rows) at the CpG island of a specific gene (column). (D) Fold enrichment (×1000) of active histone mark H3K4me3 (green bars), and repressive histone marks H3K9me3 (light red bars) and H3K27me3 (dark red bars) in the promoters of pluripotency genes by μChIP. Input samples were used for normalisation, and control IgGs were used as a reference for fold-enrichment calculation using the $2^{-\Delta\Delta Ct}$ method.

Expression of SC markers and transcription factors along the CV axis is associated with a specific histone modification pattern

We chose to study pluripotency genes (*Lgr5*, *Bmi1* and *Ascl2)* and genes encoding transcription factors (*Cdx2*) in which we had found CpG islands in the 3 kb region upstream their transcription or translation start site (Fig. S1) either with MethPrimer (Li & Dahiya, 2002) or in the UCSC Genome Browser (Kent et al., 2002). For μChIP, we chose three histone modifications known to be involved during development and embryonic SC differentiation in mammals: H3K9me3 and H3K27me3 involved in the silencing of genes that are irrelevant to the lineage in which the cells are engaged (Loh et al., 2007; Shen et al., 2008) and H3K4me3 which is essential for the expression of specific differentiation markers.

DNA methylation was absent from *Lgr5*, *Bmi1* and *Ascl2* promoters regardless of the position in the CV axis (Fig. 2C). The active histone mark H3K4me3 was enriched at *Lgr5* promoter exclusively in the crypts (Fig. 2D), where *Lgr5* is expressed (Fig. 2A). The highest enrichment for the two repressive marks H3K9me3 and H3K27me3 were found at the CV junction and in the villi (Fig. 2D),

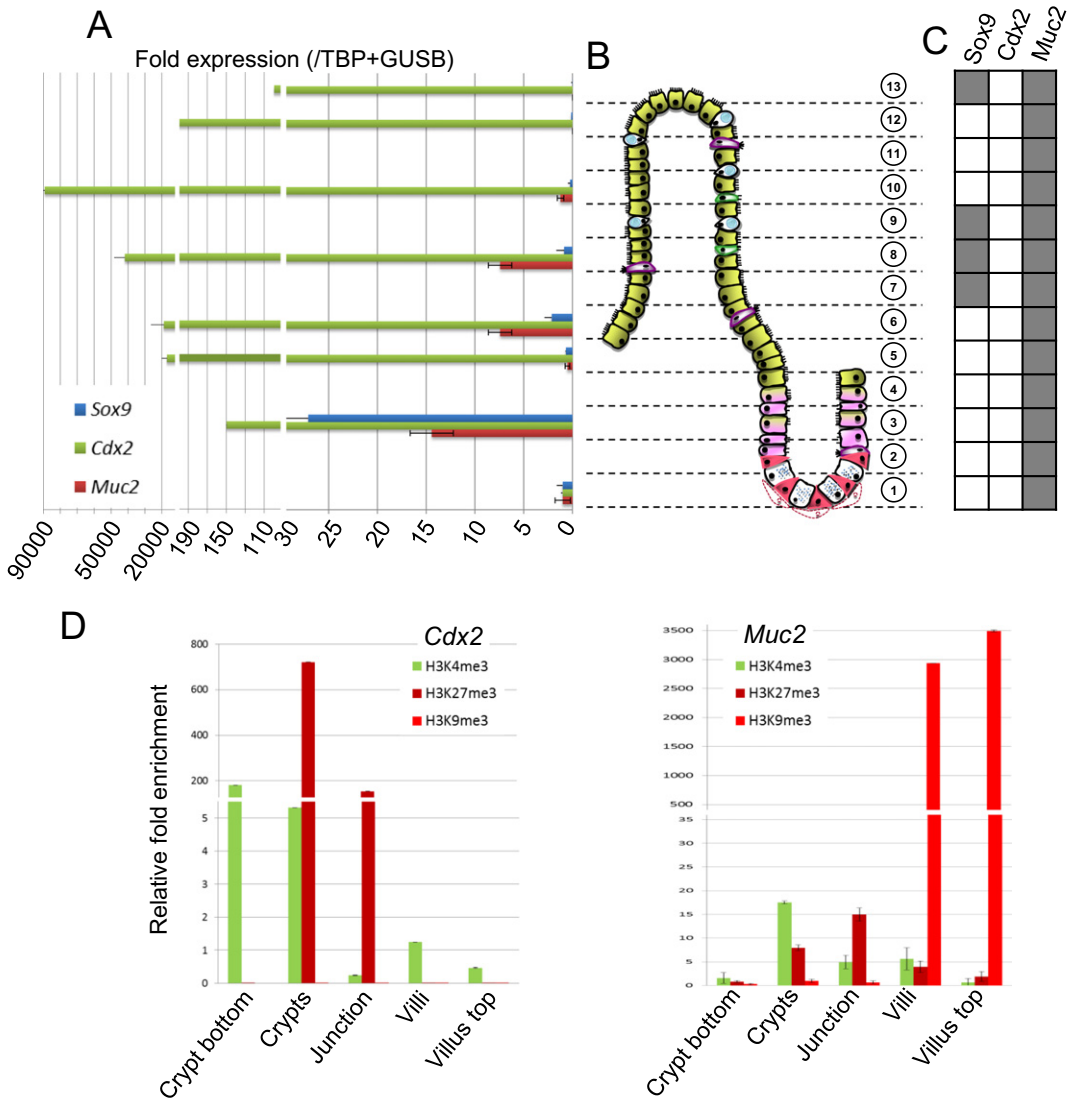

Figure 3 Transcriptional and epigenetic profile of transcription factors and differentiation markers along the CV axis. (A) Expression profile in each layer of the CV axis of one tissue block was studied by qRT-PCR. Graphs represent relative expression normalised with the housekeeping genes *GUSB* and *TBP*. The sample corresponding to the bottom of the crypt was used as a reference and fold changes were calculated according to the $2^{-\Delta\Delta Ct}$ method. (B) Schematic representation of the intestinal mucosa delineated into the 13 40 μm-layers of the CV axis that were used either for mRNA expression, MSP or ChIP analysis. (C) DNA methylation profile in each layer of the CV axis at promoters of differentiation markers was studied by MSP. White boxes indicate the absence of DNA methylation in a layer (rows) at the CpG island of a specific gene (column). Grey boxes indicate partial methylation. (D) Fold enrichment (×1000) of active histone mark H3K4me3 (green bars), and repressive histone marks H3K9me3 (light red bars) and H3K27me3 (dark red bars) in the promoters of differentiation markers by μChIP. Input samples were used for normalisation and control IgGs were used as a reference for fold-enrichment calculation using the $2^{-\Delta\Delta Ct}$ method.

where *Lgr5* shows low or no expression (Fig. 2A). Hence, there is a good correlation between *Lgr5* expression profile and the presence of active histone marks in the crypt. Interestingly, the promoters of *Lgr5*, *Bmi1* and *Ascl2* harboured chromatin bivalency (presence of both active and repressive histone marks) in the higher crypts (*Lgr5*, *Bmi1*), at the CV junction and in the lower villi (*Bmi1*) or in the entire crypts (*Ascl2*). *Lgr5* and *Ascl2* promoters were enriched exclusively with repressive marks in the villi. At the top of the villi, the three promoters were enriched exclusively with H3K9me3 and H3K27me3 (Fig. 2D).

Similarly, *Cdx2* CpG island was not methylated regardless of the depth in the CV axis. It was enriched with both H3K4me3 and H3K27me3 in the higher crypts and at the CV junction where progenitor cells are located (Fig. 3D). At the bottom of the crypt, where *Cdx2*-expressing Paneth cells are located, we were only able to observe an enrichment of H3K4me3. Similarly, in the villi, where *Cdx2* transcripts were mostly found (Fig. 3A), *Cdx2* CpG island was exclusively associated with H3K4me3. It has already been suggested that Suz12, a member of the PcG complex overexpressed in the crypts where it catalyses H3K27me3, may inhibit cell differentiation by silencing *Cdx2* expression (Benoit et al.,

2012). Here we confirm the presence of this repressive histone mark exclusively in the progenitor cell compartment and therefore further endorse the crucial role of this transcription factor in the regulation of terminal epithelial differentiation in the intestine. Moreover, Cdx2 contributes to the establishment and maintenance of the active mark H3K4me3 (Verzi et al., 2013), pointing out the interconnections between epigenetic regulation and transcription factors upon differentiation.

Bivalency has been first described in ESC at "poised" genes, ready to respond to differentiation signals (Bernstein et al., 2006). Interestingly, the ISC marker Bmi1 has been shown to play a critical role in this mechanism in adult SC and progenitors (Oguro et al., 2010). This bivalency could be due to different allelic states (Tollervey & Lunyak, 2012) or cell heterogeneity as it may be the case for *Muc2* promoter where mixed enterocytes and goblet cells induce partial methylation (Gratchev et al., 2001). However, the fact that not all promoters at the bottom of the crypt harbour this bivalency suggests that there is a real progression in epigenetic profiles along the CV axis and that SC and differentiated cells located at the bottom of the crypt may share some epigenetic features. This will have to be further validated using single cell approaches such as ISH-PLA (Gomez et al., 2013). This is interesting since it has been hypothesised that Paneth cells would derive from specific progenitors that are able to revert back into Lgr5+ SC while the rest of the intestinal epithelial cells derive from other progenitors after multiple cycling (Clevers, 2013b). Therefore, other differentiated cells may be epigenetically more distant from the SC of origin than Paneth cells. This points out the relevance of studying epigenetic profiles as a progression along the CV axis rather than in sorted cells where they are separated essentially on the basis of their terminal phenotype. This confirms the relevance of our method in addition to other approaches when it comes to genome-wide studies.

Sox9 promoter is associated with partial DNA demethylation only in the villi

We then studied the DNA methylation profile of the CpG island found in the promoter of *Sox9*, which encodes a transcription factor involved both in SC maintenance and establishment of the secretory lineage (Blache et al., 2004). Interestingly, *Sox9* promoter was totally unmethylated in the crypts where it is the most highly expressed (Fig. 3A, layer 3, and Ramalingam et al., 2012) but was found partially methylated in some cryosections corresponding to the villi and at the top of the villi (Fig. 3C). Hence, DNA methylation may be responsible for the absence of *Sox9* expression only in terminally differentiated enterocytes, which represent 90% of the villus epithelial cell contingency. Since *Sox9* has been recently described as a marker of the fifth type of intestinal epithelial cells, the Tuft cells (Gerbe et al., 2011), the absence of methylation in some layers or the fact that we were able to only show partial methylation in the villi may be due to the presence of these rare *Sox9*-expressing cells unequally distributed all along the villi. *SOX9* promoter has been described as hypermethylated in several cancer types but, to our knowledge, its methylation profile has not been studied in normal intestinal cells so far.

Expression of Muc2 along the CV axis is associated both with a specific histone code and DNA methylation profile

We found that the promoter of *Muc2*, encoding the main goblet cell marker, was partially methylated in almost all layers along the CV axis (Fig. 3C). Partial methylation of *Muc2* promoter has already been reported in human colon where the percentage of microdissected goblet cells has been shown to interfere with the percentage of *MUC2* CpG island methylation (Gratchev et al., 2001). Interestingly, no methylation was observed at the bottom of the crypt, where *Muc2* transcripts were found the most abundant (Fig. 3A). Following the same epigenetic pattern along the CV axis, low enrichment was found for repressive histone marks at the bottom of the crypts while *Muc2* promoter was enriched with H3K27me3 and/or H3K9me3 from the crypt junction to the top of the villi, indicating that most of the differentiated cells present in the villi (*i.e.* enterocytes) harbour a silenced *Muc2* promoter characterised by a high percentage of methylation and a repressive histone code. Concordant with the high expression of *Muc2* in the crypts, the highest enrichment for H3K4me3 was found in this compartment. We and others have previously described epigenetic regulation of *Muc2* in several cancer types. This suggests that the same epigenetic mechanisms are involved in *Muc2* (and *Sox9*) regulation in normal and cancer cells. On the contrary, DNA hyper- or hypomethylation of *Cdx2* and SC markers has not been described in normal tissues and seems to be cancer-specific (Kawai et al., 2005; Kwon et al., 2013). It has been suggested that aberrant DNA methylation observed in cancer may be associated with a bivalency state observed in SC (Rodriguez et al., 2008). Further investigation associating our cryosectioning model with epigenome-wide studies will be of great interest to answer this yet unsolved question.

Altogether, our data indicate that terminal differentiation markers are specifically regulated by DNA methylation and histone modifications while most of the other genes are regulated by histone modifications. Further studies, including the analysis of methylation profiles of differentiation markers that do not harbour a CpG island, will be necessary to confirm this hypothesis in our model since these regions have been shown to play an important role in cell differentiation (Miranda & Jones, 2007). Nonetheless, our results are in total accordance with other epigenome-wide studies showing that healthy adult cells acquire only a few changes in DNA methylation profiles, affecting only a small percentage of tissue-specific genes (around 6%), upon differentiation (Berdasco & Esteller, 2011). This is especially true in healthy intestinal tissues where bisulfite sequencing studies have shown that DNA methylation profiles are particularly stable (Kaaij et al., 2013).

Interestingly, we found a very good correlation between the expression profile of studied genes and their histone modification pattern, hence validating our hypothesis of epigenetic mechanisms playing crucial roles in the establishment of intestinal cell differentiation (Vincent & Van

Seuningen, 2009) and validating our strategy along the CV axis.

Conclusion

Both our expression data, which are concordant with previously found gradient profiles along the CV axis, and our epigenetic profile studies, which are in accordance with current knowledge about epigenetic mechanisms in normal differentiating cells, validate our method. Our results, obtained with semi-quantitative methods, such as MSP, allow us to consider using more sensitive and quantitative techniques to decipher epigenome-wide regulation of intestinal and colonic cell differentiation. Moreover, unlike cell sorting assays, our direct *ex vivo* method on fixed tissues, which does not involve a dissociation step, does not alter epigenetic profiles and is easier to set up. It will allow us to section out, capture and map gradual epigenetic progressions along the CV axis. This method is also a great additional asset to assess whether there is a rapid switch in epigenetic profiles in transit amplifying progenitor cells as they migrate and engage into a particular cell fate under the influence of neighbouring cells (Kim et al., 2014). Finally, as carcinogenesis is described as a dedifferentiation (reprogramming of differentiated cells) or a dysdifferentiation (aberrant programming of SC) process (Vincent & Van Seuningen, 2012), unravelling the epigenetic mechanisms accompanying normal cell differentiation using this method will be particularly useful to understand the aberrant epigenetic alterations universally observed in tumours.

Supplementary data to this article can be found online at http://dx.doi.org/10.1016/j.scr.2014.12.002.

Acknowledgments

Dr A. Vincent has received funding from the Fondation ARC and the Région Nord-Pas de Calais. This work is supported by a grant from the Ligue Nationale Contre le Cancer-Comité de l'Oise, the Gefluc-Flandres, the "Contrat de Plan Etat Région" (CPER 2007-2013, IVS). We thank the animal facility from the IFR114/IMPRT, University of Lille 2 (D. Taillieu).

References

Allegrucci, C., Wu, Y.Z., Thurston, A., et al., 2007. Restriction landmark genome scanning identifies culture-induced DNA methylation instability in the human embryonic stem cell epigenome. Hum Mol Genet 16 (10), 1253–1268. http://dx.doi.org/10.1093/hmg/ddm074 (ddm074 [pii]).

Barker, N., van Es, J.H., Kuipers, J., et al., 2007. Identification of stem cells in small intestine and colon by marker gene Lgr5. Nature 449 (7165), 1003–1007. http://dx.doi.org/10.1038/nature06196 (nature06196 [pii]).

Barnard, J.A., Beauchamp, R.D., Coffey, R.J., Moses, H.L., 1989. Regulation of intestinal epithelial cell growth by transforming growth factor type beta. Proc Natl Acad Sci U S A 86 (5), 1578–1582 (Available at: http://www.pubmedcentral.nih.gov/articlerender.fcgi?artid=286741&tool=pmcentrez&rendertype=abstract. Accessed September 2, 2014).

Benoit, Y.D., Paré, F., Francoeur, C., et al., 2010. Cooperation between HNF-1alpha, Cdx2, and GATA-4 in initiating an enterocytic differentiation program in a normal human intestinal epithelial progenitor cell line. Am J Physiol Gastrointest Liver Physiol 298 (4), G504–G517. http://dx.doi.org/10.1152/ajpgi.00265.2009.

Benoit, Y.D., Lepage, M.B., Khalfaoui, T., et al., 2012. Polycomb repressive complex 2 impedes intestinal cell terminal differentiation. J Cell Sci 125 (Pt 14), 3454–3463. http://dx.doi.org/10.1242/jcs.102061.

Berdasco, M., Esteller, M., 2011. DNA methylation in stem cell renewal and multipotency. Stem Cell Res Ther 2 (5), 42. http://dx.doi.org/10.1186/scrt83.

Bernstein, B.E., Mikkelsen, T.S., Xie, X., et al., 2006. A bivalent chromatin structure marks key developmental genes in embryonic stem cells. Cell 125 (2), 315–326. http://dx.doi.org/10.1016/j.cell.2006.02.041 (S0092-8674(06)00380-1 [pii]).

Bibikova, M., Chudin, E., Wu, B., et al., 2006. Human embryonic stem cells have a unique epigenetic signature. Genome Res 16 (9), 1075–1083. http://dx.doi.org/10.1101/gr.5319906 (gr.5319906 [pii]).

Blache, P., van de Wetering, M., Duluc, I., et al., 2004. SOX9 is an intestine crypt transcription factor, is regulated by the Wnt pathway, and represses the CDX2 and MUC2 genes. J Cell Biol 166 (1), 37–47 (Available at: http://www.ncbi.nlm.nih.gov/entrez/query.fcgi?cmd=Retrieve&db=PubMed&dopt=Citation&list_uids=15240568).

Buisine, M.P., Devisme, L., Maunoury, V., et al., 2000. Developmental mucin gene expression in the gastroduodenal tract and accessory digestive glands. I. Stomach. A relationship to gastric carcinoma. J Histochem Cytochem 48 (12), 1657–1666 (Available at: http://www.ncbi.nlm.nih.gov/entrez/query.fcgi?cmd=Retrieve&db=PubMed&dopt=Citation&list_uids=11101634).

Chawengsaksophak, K., James, R., Hammond, V.E., Kontgen, F., Beck, F., 1997. Homeosis and intestinal tumours in Cdx2 mutant mice. Nature 386 (6620), 84–87 (Available at: http://www.ncbi.nlm.nih.gov/entrez/query.fcgi?cmd=Retrieve&db=PubMed&dopt=Citation&list_uids=9052785).

Clevers, H., 2013a. The intestinal crypt, a prototype stem cell compartment. Cell 154 (2), 274–284. http://dx.doi.org/10.1016/j.cell.2013.07.004.

Clevers, H., 2013b. Stem cells: a unifying theory for the crypt. Nature 495 (7439), 53–54. http://dx.doi.org/10.1038/nature11958.

Gerbe, F., van Es, J.H., Makrini, L., et al., 2011. Distinct ATOH1 and Neurog3 requirements define tuft cells as a new secretory cell type in the intestinal epithelium. J Cell Biol 192 (5), 767–780. http://dx.doi.org/10.1083/jcb.201010127.

Gomez, D., Shankman, L.S., Nguyen, A.T., Owens, G.K., 2013. Detection of histone modifications at specific gene loci in single cells in histological sections. Nat Methods 10 (2), 171–177. http://dx.doi.org/10.1038/nmeth.2332.

Gratchev, A., Siedow, A., Bumke-Vogt, C., et al., 2001. Regulation of the intestinal mucin MUC2 gene expression in vivo: evidence for the role of promoter methylation. Cancer Lett 168 (1), 71–80 (Available at: http://www.ncbi.nlm.nih.gov/entrez/query.fcgi?cmd=Retrieve&db=PubMed&dopt=Citation&list_uids=11368880).

Grossmann, J., Walther, K., Artinger, M., Rümmele, P., Woenckhaus, M., Schölmerich, J., 2002. Induction of apoptosis before shedding of human intestinal epithelial cells. Am J Gastroenterol 97 (6), 1421–1428. http://dx.doi.org/10.1111/j.1572-0241.2002.05787.x.

Ho, L.-L., Sinha, A., Verzi, M., Bernt, K.M., Armstrong, S.A., Shivdasani, R.A., 2013. DOT1L-mediated H3K79 methylation in chromatin is dispensable for Wnt pathway-specific and other intestinal epithelial functions. Mol Cell Biol 33 (9), 1735–1745. http://dx.doi.org/10.1128/MCB. 01463-12.

Itzkovitz, S., Lyubimova, A., Blat, I.C., et al., 2012. Single-molecule transcript counting of stem-cell markers in the mouse intestine.

Nat Cell Biol 14 (1), 106–114. http://dx.doi.org/10.1038/ncb2384.

Kaaij, L.T., van de Wetering, M., Fang, F., et al., 2013. DNA methylation dynamics during intestinal stem cell differentiation reveals enhancers driving gene expression in the villus. Genome Biol 14 (5), R50. http://dx.doi.org/10.1186/gb-2013-14-5-r50.

Kawai, H., Tomii, K., Toyooka, S., et al., 2005. Promoter methylation downregulates CDX2 expression in colorectal carcinomas. Oncol Rep 13 (3), 547–551 (Available at: http://www.ncbi.nlm.nih.gov/entrez/query.fcgi?cmd=Retrieve&db=PubMed&dopt=Citation&list_uids=15706431).

Kent, W.J., Sugnet, C.W., Furey, T.S., et al., 2002. The human genome browser at UCSC. Genome Res 12 (6), 996–1006. http://dx.doi.org/10.1101/gr.229102 (Article published online before print in May 2002).

Kim, T.-H., Li, F., Ferreiro-Neira, I., et al., 2014. Broadly permissive intestinal chromatin underlies lateral inhibition and cell plasticity. Nature 506 (7489), 511–515. http://dx.doi.org/10.1038/nature12903.

Kwon, O.-H., Park, J.-L., Baek, S.-J., et al., 2013. Aberrant upregulation of ASCL2 by promoter demethylation promotes the growth and resistance to 5-fluorouracil of gastric cancer cells. Cancer Sci 104 (3), 391–397. http://dx.doi.org/10.1111/cas.12076.

Li, L.-C., Dahiya, R., 2002. MethPrimer: designing primers for methylation PCRs. Bioinformatics 18 (11), 1427–1431 (Available at: http://www.ncbi.nlm.nih.gov/pubmed/12424112. Accessed September 3, 2014).

Loh, Y.H., Zhang, W., Chen, X., George, J., Ng, H.H., 2007. Jmjd1a and Jmjd2c histone H3 Lys 9 demethylases regulate self-renewal in embryonic stem cells. Genes Dev 21 (20), 2545–2557. http://dx.doi.org/10.1101/gad.1588207 (21/20/2545 [pii]).

Miranda, T.B., Jones, P.A., 2007. DNA methylation: the nuts and bolts of repression. J Cell Physiol 213 (2), 384–390. http://dx.doi.org/10.1002/jcp.21224.

Mori-Akiyama, Y., van den Born, M., van Es, J.H., et al., 2007. SOX9 is required for the differentiation of Paneth cells in the intestinal epithelium. Gastroenterology 133 (2), 539–546 (Available at: http://www.ncbi.nlm.nih.gov/entrez/query.fcgi?cmd=Retrieve&db=PubMed&dopt=Citation&list_uids=17681175).

Oguro, H., Yuan, J., Ichikawa, H., et al., 2010. Poised lineage specification in multipotential hematopoietic stem and progenitor cells by the polycomb protein Bmi1. Cell Stem Cell 6 (3), 279–286. http://dx.doi.org/10.1016/j.stem.2010.01.005.

Pennarossa, G., Maffei, S., Campagnol, M., Tarantini, L., Gandolfi, F., Brevini, T.A.L., 2013. Brief demethylation step allows the conversion of adult human skin fibroblasts into insulin-secreting cells. Proc Natl Acad Sci U S A 110 (22), 8948–8953. http://dx.doi.org/10.1073/pnas.1220637110.

Ramalingam, S., Daughtridge, G.W., Johnston, M.J., Gracz, A.D., Magness, S.T., 2012. Distinct levels of Sox9 expression mark colon epithelial stem cells that form colonoids in culture. Am J Physiol Gastrointest Liver Physiol 302 (1), G10–G20. http://dx.doi.org/10.1152/ajpgi.00277.2011.

Rodriguez, J., Muñoz, M., Vives, L., Frangou, C.G., Groudine, M., Peinado, M.A., 2008. Bivalent domains enforce transcriptional memory of DNA methylated genes in cancer cells. Proc Natl Acad Sci U S A 105 (50), 19809–19814. http://dx.doi.org/10.1073/pnas.0810133105.

Sangiorgi, E., Capecchi, M.R., 2008. Bmi1 is expressed in vivo in intestinal stem cells. Nat Genet 40 (7), 915–920. http://dx.doi.org/10.1038/ng.165 (ng.165 [pii]).

Scoville, D.H., Sato, T., He, X.C., Li, L., 2008. Current view: intestinal stem cells and signaling. Gastroenterology 134 (3), 849–864. http://dx.doi.org/10.1053/j.gastro.2008.01.079 (S0016-5085(08)00185-6 [pii]).

Sheaffer, K.L., Kim, R., Aoki, R., et al., 2014. DNA methylation is required for the control of stem cell differentiation in the small intestine. Genes Dev 28 (6), 652–664. http://dx.doi.org/10.1101/gad.230318.113.

Shen, X., Liu, Y., Hsu, Y.J., et al., 2008. EZH1 mediates methylation on histone H3 lysine 27 and complements EZH2 in maintaining stem cell identity and executing pluripotency. Mol Cell 32 (4), 491–502. http://dx.doi.org/10.1016/j.molcel.2008.10.016 (S1097-2765(08)00732-6 [pii]).

Tollervey, J.R., Lunyak, V.V., 2012. Epigenetics: judge, jury and executioner of stem cell fate. Epigenetics 7 (8), 823–840. http://dx.doi.org/10.4161/epi.21141.

Tytgat, K.M., Buller, H.A., Opdam, F.J., Kim, Y.S., Einerhand, A.W., Dekker, J., 1994. Biosynthesis of human colonic mucin: Muc2 is the prominent secretory mucin. Gastroenterology 107 (5), 1352–1363 (doi: S0016508594003318 [pii]).

Verzi, M.P., Shin, H., San Roman, A.K., Liu, X.S., Shivdasani, R.A., 2013. Intestinal master transcription factor CDX2 controls chromatin access for partner transcription factor binding. Mol Cell Biol 33 (2), 281–292. http://dx.doi.org/10.1128/MCB.01185-12.

Vincent, A., Van Seuningen, I., 2009. Epigenetics, stem cells and epithelial cell fate. Differentiation 78 (2-3), 99–107. http://dx.doi.org/10.1016/j.diff.2009.07.002 (S0301-4681(09)00083-8 [pii]).

Vincent, A., Van Seuningen, I., 2012. On the epigenetic origin of cancer stem cells. Biochim Biophys Acta 1826 (1), 83–88. http://dx.doi.org/10.1016/j.bbcan.2012.03.009 (S0304-419X(12)00023-6 [pii]).

Vincent, A., Omura, N., Hong, S.-M., Jaffe, A., Eshleman, J., Goggins, M., 2011. Genome-wide analysis of promoter methylation associated with gene expression profile in pancreatic adenocarcinoma. Clin Cancer Res 17 (13), 4341–4354.

Wang, F., Scoville, D., He, X.C., et al., 2013. Isolation and characterization of intestinal stem cells based on surface marker combinations and colony-formation assay. Gastroenterology 145 (2), 383–395.e1-21. http://dx.doi.org/10.1053/j.gastro.2013.04.050.